Supporting Information for:

Comparison of data-driven and general temporal constraints on compressed sensing for breast DCE MRI

Ping N Wang[1], Julia V Velikina[1], Roberta M Strigel[1,2,3], Leah C Henze Bancroft[2],

Alexey A Samsonov[2], Ty A Cashen[4], Kang Wang[4], Frederick Kelcz[2], Kevin M Johnson[1,2],

Frank R Korosec[2], Ali Ersoz[5], and James H Holmes[2]

[1]Department of Medical Physics, University of Wisconsin-Madison School of Medicine and Public Health, Madison, WI, United States,

[2]Department of Radiology, University of Wisconsin-Madison School of Medicine and Public Health, Madison, WI, United States,

[3]Carbone Cancer Center, University of Wisconsin-Madison, Madison, WI, United States,

[4]Global MR Applications & Workflow, GE Healthcare, Madison, WI, United States,

[5]MR Engineering, GE Healthcare, Waukesha, WI, United States

	K^{trans}	V_e	V_p	Simulated Lesion Type
Lesion 1	0.430	0.620	0.06	Intermediate
Lesion 2	0.280	0.633	0.06	Intermediate
Lesion 3	0.321	0.137	0.0153	Malignant
Lesion 4	0.122	0.137	0.0153	Benign
Lesion 5	0.515	0.137	0.0153	Malignant
Lesion 6	0.082	0.137	0.0153	Benign
Lesion 7	0.062	0.137	0.0153	Benign

Supporting Information Table S1. Simulated pharmacokinetic (PK) parameters for each lesion in the Digital Reference Objects (DROs). PK parameters for different lesion types are simulated based on the reference: ACR BI-RADS Breast Magnetic Resonance Imaging[1] and chosen to correspond to expected malignant, benign, and intermediate lesion kinetics in breast cancers. An image depicting the lesion locations and the corresponding concentration-time curves are shown in Figure 1 of the main document.
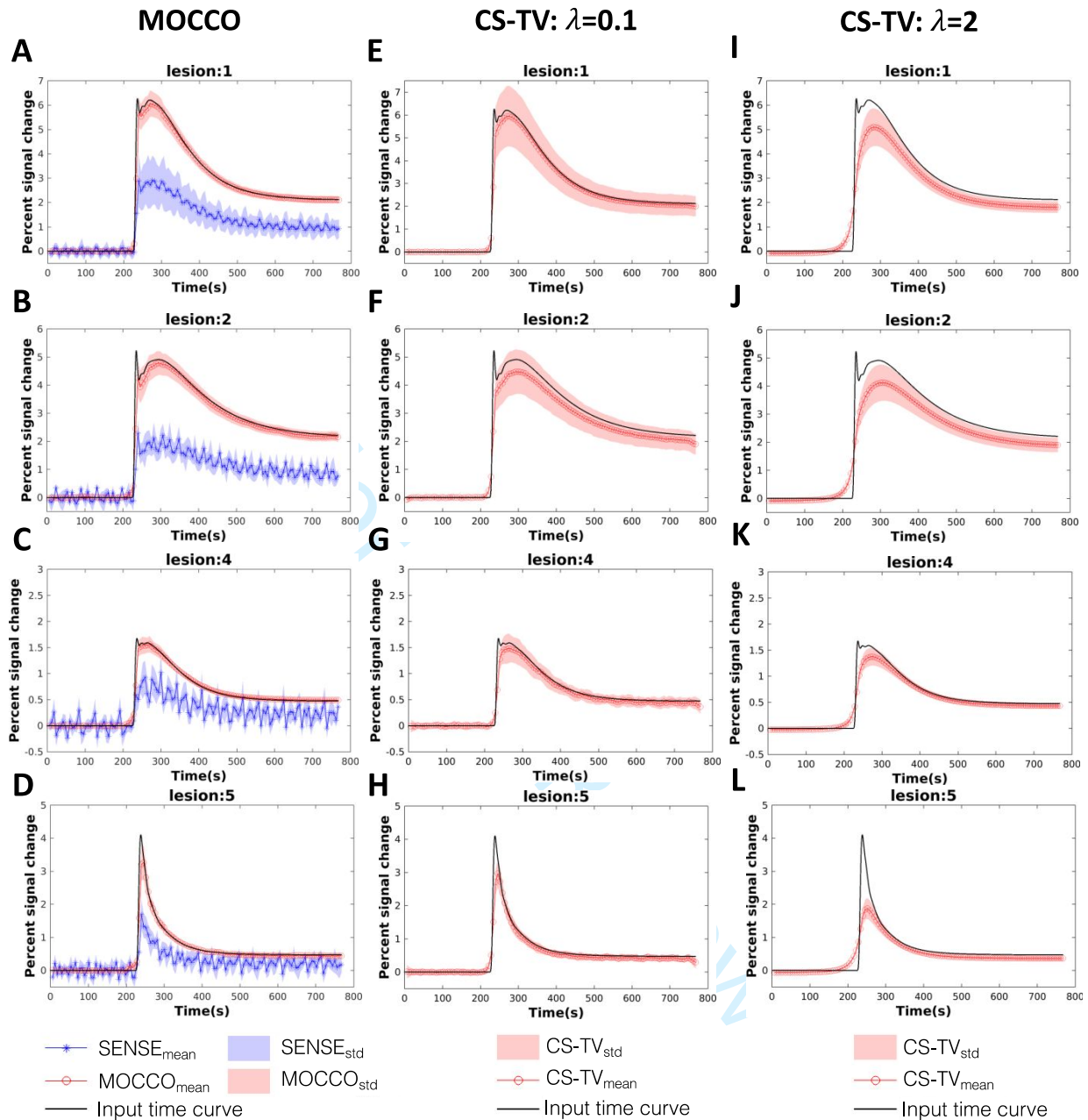
Supporting Information Figure S1. Simulated contrast agent uptake curves plotted for the time interval of 0 s to 720 s, including pre-contrast and post-contrast wash-out phases. Mean percent signal change measured in four uniquely enhancing 8 mm lesions (lesions 1, 2, 4 and 5 as defined in Figure 1) reconstructed using MOCCO (A-D, red circles), CS-TV with λ = 0.1 (E-H, red circles), CS-TV with λ = 2 (I-L, red circles) and iterative SENSE (A-D, blue stars). Standard deviations are shown with banded areas. The input time curves used to generate the source data are plotted with black lines in all frames.
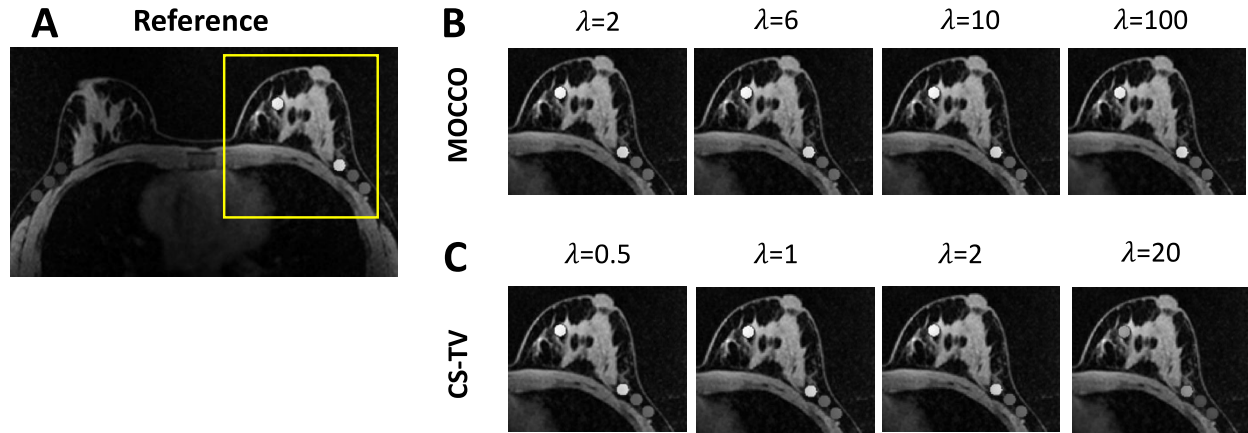
Supporting Information Figure S2. Images reconstructed from the fully sampled reference data (A), MOCCO (B), and CS-TV (C) with different values for the regularization parameter (λ). Both methods showed improved image quality when increasing λ from 0-10 for MOCCO and λ from 0-2 for CS-TV. For larger λ ($\lambda > 20$ for MOCCO and $\lambda > 6$ for CS-TV), the reconstructed images were observed to be overly smoothed and resulted in lower intensity due to over constrained reconstruction.

Additional analysis of temporal fidelity

PK modeling was performed using the ROCKETSHIP toolbox[2] by fitting the extended Tofts model to the time-signal curves using the Levenberg-Marquardt algorithm. The obtained PK parameters were then compared to the PK parameters used to generate the input time curves for the simulation to determine how well the acquisition and reconstruction could recover the time curves. The input PK parameters are listed in Supporting Information Table S1.

	Lesion #	1	2	3	4	5	6	7
Reference	K^{trans} (%)	0.18	0.24	-3.31	1.88	-7.46	1.90	1.95
	V_e (%)	-1.23	-1.55	-0.06	-0.03	0.70	-0.44	-0.18
	V_p (%)	-27.34	-23.59	-34.58	-29.00	-34.50	-24.70	-23.31
MOCCO	K^{trans} (%)	4.31	4.44	-17.54	-3.33	-30.96	-1.25	1.78
	V_e (%)	3.96	2.16	1.41	4.42	-0.38	3.65	1.01
	V_p (%)	-65.59	-60.88	-34.64	-34.64	-34.64	-34.64	-34.57
CS-TV λ= 0.1	K^{trans} (%)	-1.21	-2.11	-31.99	-11.88	-49.21	-8.59	-4.50
	V_e (%)	2.11	-1.20	-1.61	0.07	-5.95	-1.92	-0.73
	V_p (%)	-70.80	-65.65	-34.64	-34.64	-34.64	-34.64	-34.58
CS-TV λ= 2	K^{trans} (%)	-16.84	-11.93	-44.60	-19.91	-65.24	-16.98	-11.18
	V_e (%)	-4.82	-5.72	-5.51	-1.60	-13.63	-3.22	-1.57
	V_p (%)	-70.21	-69.92	-34.64	-34.64	-28.65	-34.64	-34.62

Supporting Information Table S2. Percent error (%) of PK parameters fit from the signal-time curves generated from 8 mm lesions in MOCCO, CS-TV: λ = 0.1, CS-TV: λ = 2, and the fully-sampled reference images shown in Figure 2 of the main manuscript. Fully-sampled reference images with 5 s temporal resolution showed overall accurate measurements in Ktrans and Ve (< 2%) in most lesions. Lesion 3 and 5 with the most rapid temporal enhancement showed underestimation in Ktrans, which demonstrated that this kind of sharp peak is difficult to recover by 5 s temporal resolution. Larger overall errors were also found for Vp, which matched the results in Litjens et al. [3] that suggested 5 s temporal resolution may not be sufficient to provide reliable Vp measurements. Both MOCCO and CS-TV: λ = 0.1 showed promising results in Ktrans and Ve (within 10% error range). However, underestimation was observed for both methods in lesions with the most rapid temporal enhancement (lesion 3 and 5). CS-TV: λ = 2 showed

overall higher error in Ktrans that was likely due to temporal over-smoothing of the wash-in slope. Larger overall errors were found for Vp in all reconstructions.

| Lesion size	Lesion #	1	2	3	4	5	6	7
1.5 mm	K^{trans} (%)	-3.10	-5.58	-8.42	-4.87	-13.77	-4.35	-3.55
	V_e (%)	-4.45	-7.30	-5.23	-6.36	-5.49	-5.93	-5.76
	V_p (%)	-29.62	-27.87	-34.57	-32.64	-34.63	-29.07	-27.68
5 mm	K^{trans} (%)	1.34	0.87	-1.85	1.14	-6.27	0.99	2.85
	V_e (%)	-0.10	-0.95	1.07	0.24	1.80	-0.33	0.75
	V_p (%)	-26.48	-23.03	-34.59	-27.13	-34.52	-25.21	-22.55
8 mm	K^{trans} (%)	0.18	0.24	-3.31	1.88	-7.46	1.90	1.95
	V_e (%)	-1.23	-1.55	-0.06	-0.03	0.70	-0.44	-0.18
	V_p (%)	-27.34	-23.59	-34.58	-29.00	-34.50	-24.70	-23.31
10 mm	K^{trans} (%)	0.83	0.39	-2.41	1.63	-7.16	1.91	1.76
	V_e (%)	-0.67	-1.41	-0.12	0.23	0.96	0.00	-0.51
	V_p (%)	-27.34	-23.57	-34.59	-28.63	-34.64	-24.74	-21.08

Supporting Information Table S3. Percent error (%) of the PK parameters fit from the signal-time curves generated from fully-sampled reference images. The fully-sampled reference images allowed recovery of Ktrans and Ve across lesion sizes larger than 5 mm (within 5% error range). However, underestimation of Ktrans and Ve was observed in the 1.5 mm lesion (within 10% error range). Although, larger overall error were found for Vp, the error range was consistent with the fully-sampled reference results in Table S2 across different lesion sizes. Only lesions with 1.5 mm showed increased error (~ 5% increased).

Lesion size	Lesion #	1	2	3	4	5	6	7
1.5 mm	K^{trans} (%)	3.70	0.07	-27.80	-9.61	-43.66	-0.50	3.86
	V_e (%)	1.09	-8.31	-2.58	-0.46	0.48	-9.75	-12.40
	V_p (%)	-63.34	-40.06	-34.64	-34.64	-34.64	-34.64	-34.62
5 mm	K^{trans} (%)	4.58	4.33	-25.08	-7.00	-38.55	5.25	11.01
	V_e (%)	2.38	-4.77	2.33	5.01	4.85	-2.32	-8.32
	V_p (%)	-63.12	-43.03	-34.64	-34.64	-34.64	-33.61	-34.58
8 mm	K^{trans} (%)	4.31	4.44	-17.54	-3.33	-30.96	-1.25	1.78
	V_e (%)	3.96	2.16	1.41	4.42	-0.38	3.65	1.01
	V_p (%)	-65.59	-60.88	-34.64	-34.64	-34.64	-34.64	-34.57
10 mm	K^{trans} (%)	5.78	4.84	-16.91	-2.42	-29.94	0.47	2.60
	V_e (%)	5.44	1.99	1.62	4.81	-0.31	4.64	0.85
	V_p (%)	-64.69	-60.50	-34.64	-34.64	-34.64	-34.64	-34.64

Supporting Information Table S4. Percent error (%) of PK parameters fit from the signal-time curves generated from MOCCO: λ = 10. Lesion size simulations showed consistent results across all three PK parameters for MOCCO reconstruction. MOCCO reconstruction resulted in errors of less than 6% in Ktrans and Ve across the lesion sizes greater than 5mm, which was 1% higher than the corresponding results from fully-sampled reference images. Both Ktrans and Ve from the 1.5 mm lesion showed similar errors to those from the fully-sampled reference (within 10% error range). Lesions with the fastest wash-in and wash-out (Lesions 3 and 5) showed underestimation of Ktrans, consistent with incomplete recovery of the wash-in slope. The error in Ktrans was also found to increase with decreasing lesion size. Larger overall errors were found for Vp in all lesion sizes.
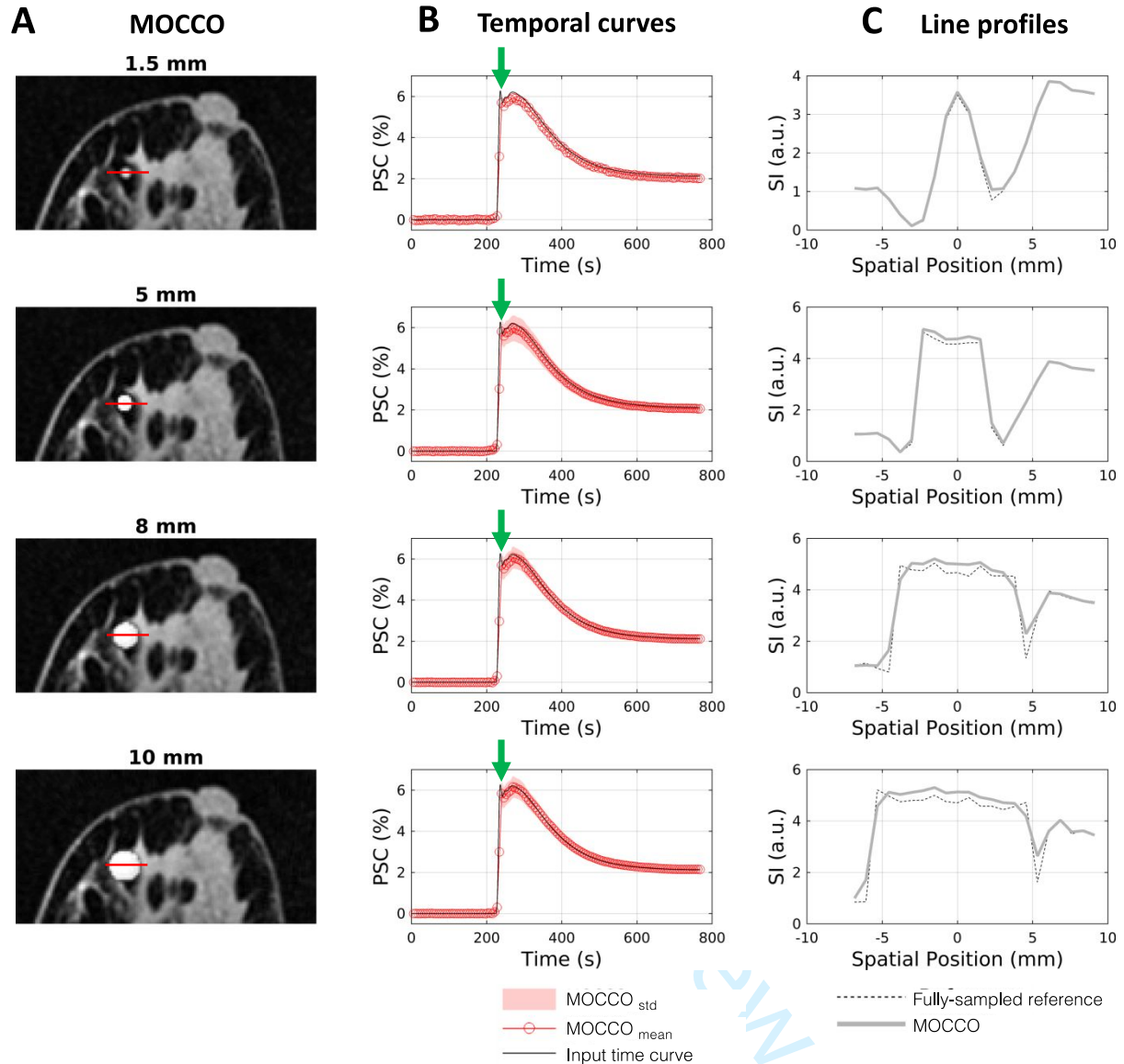
Supporting Information Figure S3. Simulation results from lesion 1 that demonstrated the highest percent signal change (PSC) compared to other lesions. Shown are example images at matched representative time frames for varying lesion size (A) along with the corresponding percent signal change time curves compared to the input time curves (B). Line profiles through the center of the lesion as indicated by the red line in (A) are plotted from undersampled data reconstructed using MOCCO (C, solid line) and the fully-sampled reference images (C, dashed line). The images (A) and line profiles (C) correspond to T = 240 s (B, green arrows).
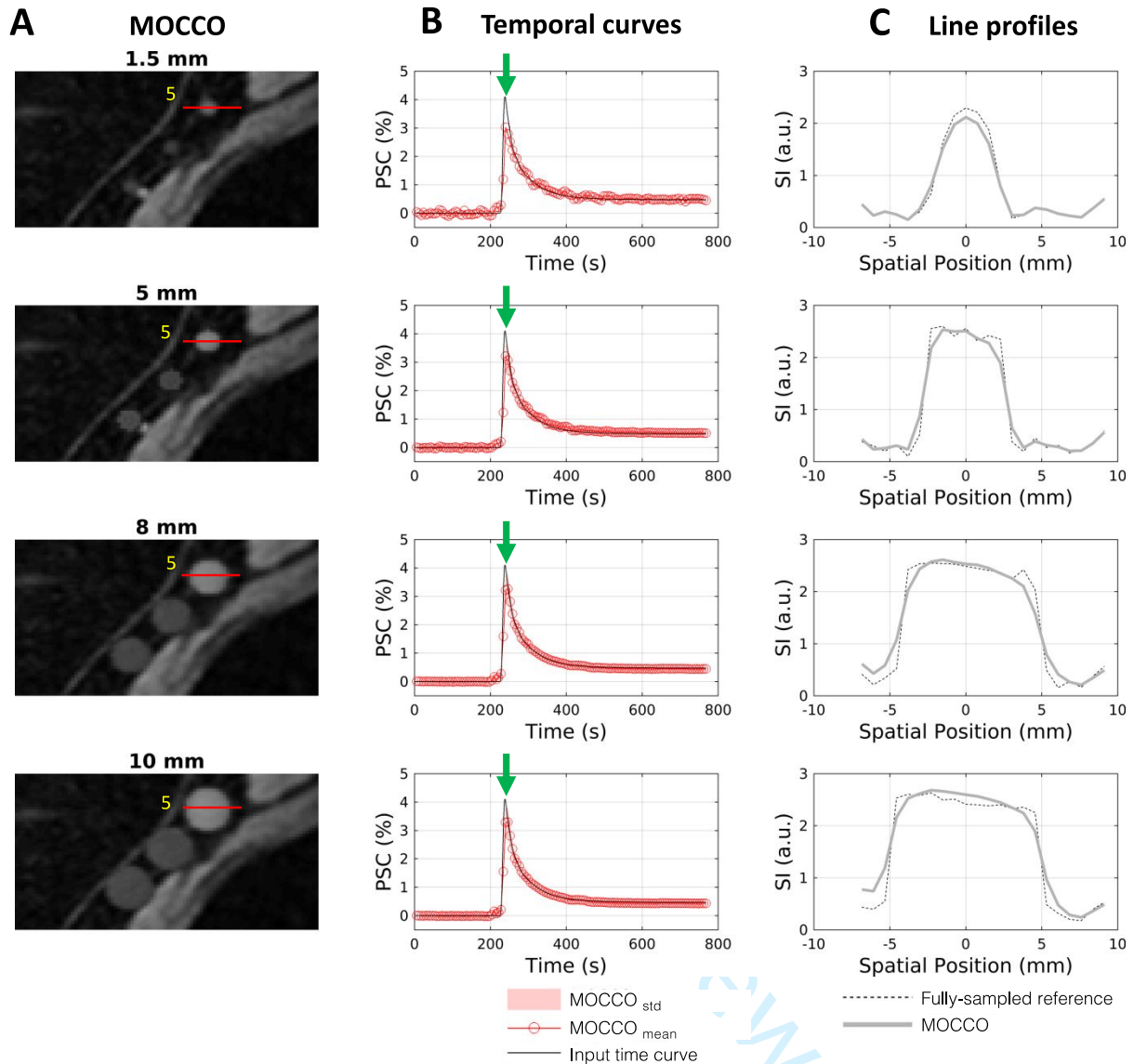
Supporting Information Figure S4. Simulation results for lesion 5 with the sharpest wash-in and wash-out contrast kinetics for different lesion sizes. A magnified region at the right side of the axilla with lesions 5 - 7 is shown for MOCCO (A). Percent signal change time curves (B) show modest temporal blurring at small lesion sizes (1.5 mm). Horizontal line profiles through the center of the lesion (red line in (A)) for reference (dashed line) and MOCCO-reconstructed (solid line) images corresponding to T = 240 s (B, green arrows).

References

1. Morris EA, Comstock CE, Lee CH. ACR BI-RADS® Magnetic Resonance Imaging. In: ACR BI-RADS® Atlas, Breast Imaging Reporting and Data System. In: *ACR BI-RADS Breast Magnetic Resonance Imaging*. American College of Radiology; 2013:18.

2. Barnes SR, Ng TSC, Santa-Maria N, Montagne A, Zlokovic BV, Jacobs RE. ROCKETSHIP: a flexible and modular software tool for the planning, processing and analysis of dynamic MRI studies. *BMC Med Imaging*. 2015;15. doi:10.1186/s12880-015-0062-3

3. Litjens GJS, Heisen M, Buurman J, ter Haar Romeny BM. Pharmacokinetic models in clinical practice: What model to use for DCE-MRI of the breast? In: *2010 IEEE International Symposium on Biomedical Imaging: From Nano to Macro*. ; 2010:185-188. doi:10.1109/ISBI.2010.5490382